

properties of Te. As emphasized in Ref. 3, the angles between the different bonds of As and Te are smaller than corresponding angles of As and, respectively, S in As_2S_3 and Se in As_2Se_3 . This property tends to produce, in vitreous $\text{As}_x\text{Te}_{100-x}$ compounds, a more compact structure which favors strong chemical interaction between As-Te₃ pyramids and hence angular distortion.

The results obtained here lead to a description of the major part of the structure in vitreous As_2S_3 and As_2Se_3 as constituting an open, locally symmetric, random covalent network, while the structure of glassy $\text{As}_x\text{Te}_{100-x}$ compounds is more close packed and thus distorted. Hence it would be interesting to reinterpret the x-ray diffraction diagrams by using the conclusions reported here. Further calculations of the EFG tensor based on atomic orbital functions might combine the σ data of this paper and the ω_Q variations given in Ref. 4 to derive fluctuations of arsenic bond angles. Finally, the method developed here can be applied to other nuclei embedded in nonoriented media and having large Q .

The authors thank P. Monod, who suggested the

experiment, and J. Cornet, who supplied all the samples used here and gave useful explanations on his own work. Laboratoire de Physique des Solides is a Laboratoire associé au Centre National de Recherches Scientifiques.

¹S. Tsuchihashi and Y. Kawamoto, *J. Non-Cryst. Solids* **5**, 286 (1971).

²A. L. Renninger and B. L. Averbach, *Phys. Rev. B* **8**, 1507 (1973).

³J. Cornet and D. Rossier, *J. Non-Cryst. Solids* **12**, 85 (1973).

⁴M. Rubinstein and P. C. Taylor, *Phys. Rev. B* **9**, 4258 (1974).

⁵S. Wada and K. Asayama, *J. Phys. Soc. Jpn.* **34**, 1163 (1973).

⁶T. P. Das and E. L. Hahn, in *Solid State Physics*, edited by F. Seitz and D. Turnbull (Academic, New York, 1958), Suppl. 1.

⁷J. Szeftel and H. Alloul, *J. Non-Cryst. Solids* **29**, 253 (1978).

⁸On the basis of chemical arguments, an isolated regular pyramid is more stable than a distorted one.

⁹At a site of octahedral symmetry, H_Q vanishes and the nuclear resonance occurs as usual at $\Omega = \gamma H$.

Lattice-Parameter Changes due to Au Dissolution in Pb

W. K. Warburton^(a) and S. C. Moss

Physics Department, University of Houston, Houston, Texas 77004

(Received 11 September 1978)

A careful measurement of the lattice parameters of pure Pb and a Pb+(0.0918 at.% Au) sample after a quench and equilibrium annealing cycle shows that Au in both monomer and "tetramer" defect states produces lattice contraction with the "tetramer" somewhat remarkably having the larger effect per atom. The observed monomer contraction suggests that the majority site occupancy for Au is substitutional and that the rapid Au diffusion must therefore involve a substitutional-interstitial mechanism.

The Pb(Au) system has been long known for its ultrafast diffusion behavior^{1,2} which has been generally considered to result from an interstitial migration mechanism.^{3,4} More recent work demonstrates that further complexity exists, with the Au forming at least three equilibrium defects having one, two, and probably four Au atoms, respectively^{5,6} (Au_1 , Au_2 , and Au_4). Actually, the existence of the Au_n , $n > 2$, defect, while not in doubt, has not been absolutely determined at $n = 4$. We here merely accept the judgment of Ref. 6 that Au_4 is the most likely candidate. Since this situation is unique among diffusion systems studied to date and since it has been demonstrated that an appropriate quench can capture the system essentially completely in the Au_4 state,^{6,7} the possibility appeared to exist that Huang diffuse

x-ray scattering⁸ might be used to obtain symmetry information about these defects. As a preliminary to such a measurement we have made a careful measurement of the change of lattice parameter, $\Delta a/a$, since this is both a measure of the strain introduced by the defects and a requirement for an estimate of the Huang scattering.

Single crystals of pure Pb and Pb+(9.18×10⁻² at.% Au) were grown by the Bridgman technique in boats of reactor-grade graphite using 99.9999%-purity Cominco Pb and 99.99%-purity Research Organic/Inorganic Chemical Corporation Au. Wafer specimens were formed by sparkcutting, following a Laue orientation to within about ½° of the [110] axis. Since Pb is particularly susceptible to surface damage, the wafers were chemically planed to obtain a flat face within about 0.05°

of the [110] with a $1/10^\circ$ rocking curve.

The wafers were oriented by their planed faces in a vacuum furnace mounted on a Rigaku diffractometer with stepping motor controls to locate θ (ω axis) and 2θ to within 0.005° . The furnace could be controlled to $\pm \frac{1}{40}^\circ\text{C}$ over periods of about 10 min. $\text{Cu } K\alpha_1$ radiation monochromatized with a bent Ge crystal was used for all measurements, giving $2\theta_{(220)} \cong 52.2$ and $2\theta_{(440)} = 123.4^\circ$.

The lattice parameters were measured using a modification of the Bond⁹ technique, required because the diffractometer could not reach -123° . Thus the (220) reflection was measured at both positive and negative values of 2θ , together with the change in ω between them. From these values the true $\theta=0$ position and the offset of the crystal face from the diffractometer axis could be computed. These are the major sources of error in the measurement and can be used to correct the value of 2θ from the (440) reflection, which is less sensitive to these errors and which, in turn, yields the lattice parameter. In the normal Bond procedure, ω is measured. Using the present

furnace it was necessary to monitor 2θ with ω being adjusted to maximize the intensity of the reflection. This procedure proved to be stable through all the various temperature cycles. The centers of the diffracted beam profiles in 2θ were found by making parabolic fits separately to both sides of the diffraction profile, in the vicinity of 80% of the maximum, interpolating to exactly 80%, and locating the mean of the two as an estimate of the ($K\alpha_1$) peak center.

Following procedures developed in Ref. 7, complete dissolution was obtained by annealing at 215°C for 30 min in a silicone oil bath with bubbled argon. The samples were then quenched into silicone oil at 20°C . This quench has been shown to be rapid enough to result in complete formation of the nominal Au_4 state without introducing precipitation centers. Consequently the alloys can remain in this metastable condition reliably for several days.

An initial set of measurements was made on pure Pb to establish a reference lattice parameter and check the experimental technique. The result was

$$a_{\text{pb}}(T) = (4.95034 \pm 0.00009)[1 + (2.879 \pm 0.014) \times 10^{-5}(T - 24) + (1.08 \pm 0.06) \times 10^{-8}(T - 24)^2] \quad (1)$$

in angstroms, T is in $^\circ\text{C}$, and uncertainties are standard-error estimates from the least-squares-fitting routine. Both lattice parameter and linear expansion coefficient are in agreement with handbook values.¹⁰ From the essentially random scatter of data points about this fit we estimate the standard deviation in the measurements themselves as $\sigma_a = 0.5 \times 10^{-4} \text{ \AA}$. The scatter in the alloy data is substantially smaller than this.

The Pb(Au) lattice parameter was first measured at room temperature following the quench described above, after which a sequence of isothermal anneals was begun (open circles on Fig. 1) to 95°C , where precipitation should precede to within 37% ($1/e$) of completion in about 77 min.⁷ After 60 min the system was measured, raised to 128°C ($1/e \sim 7$ min) for 50 min to complete precipitation, measured, and returned to 95°C to begin an equilibrium scan (squares with dot in Fig. 1). Three points were measured and the system returned to room temperature overnight. The next day a complete scan (filled circles in Fig. 1) to 226°C and back was carried out, with alternate points taken on the T increasing and decreasing legs of the scan. Several $1/e$ times were allowed for equilibration at all temperatures. Since point-defect densities are thermodynamically deter-

mined in equilibrium, the agreement between the two sets of data implies both that equilibrium was achieved and that the defect concentrations obtained in this sequence are insensitive to the sample microstructure. Surprisingly, we found that

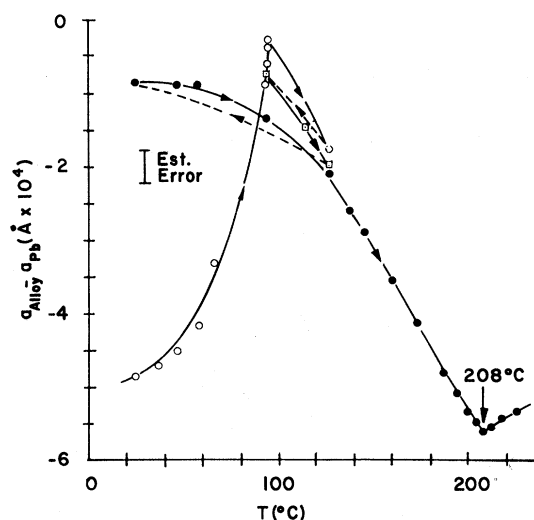


FIG. 1. Differences in lattice parameter between Pb (900 ppm Au) alloy and pure Pb as a function of temperature for the annealing schedule described in the text.

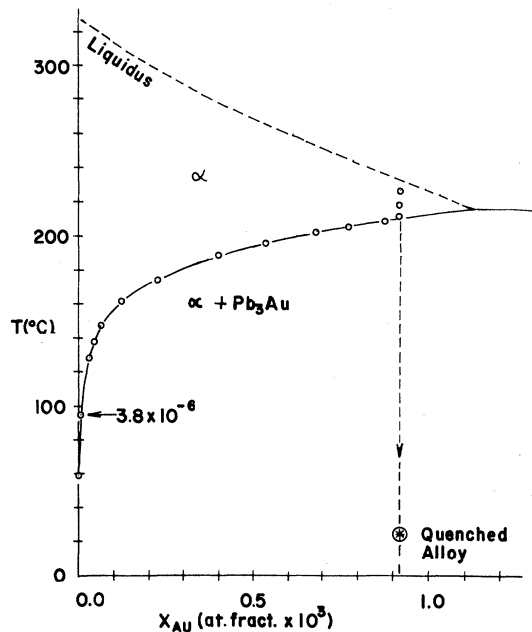


FIG. 2. An expanded section of the Pb-Au phase diagram for extremely low Au concentrations (from Rosolimo and Turnbull, Ref. 7). The points shown correspond to the equilibrium measurements shown in Fig. 1 (filled circles).

full equilibrium had only been achieved for the last point of the previous day.

We next consider Fig. 2, an expanded section of the Pb(Au) phase diagram, which shows the solid solubility of Au in Pb.⁷ For increasing temperature we see Au solubility increasing exponentially [$H_{\text{soln}} = 16.92$ kcal/mole (Ref. 7)] until the full alloy concentration is reached at 208°C, after which the system proceeds vertically into the single-phase field. The corresponding lattice-parameter behavior (filled circles in Fig. 1) is a monotonic decrease until 208°C is reached, followed by a discontinuous change in slope as the last precipitate disappears.

The first consequence of Fig. 1, from the room-temperature quench measurement, is that the fully quenched alloy is contracted relative to pure Pb at the same temperature. Two earlier measurements on separate samples showed this value of $\Delta a \sim 5 \times 10^{-4}$ Å to be quite reproducible. If this quench successfully produces a completely Au_4 distribution of gold, the $\Delta a/a$ per atom can be obtained as

$$\frac{\Delta a/a}{x_{\text{pb}}} = \frac{-4.8 \times 10^{-4}}{(4.95)(9.18 \times 10^{-4})} = -0.107. \quad (2)$$

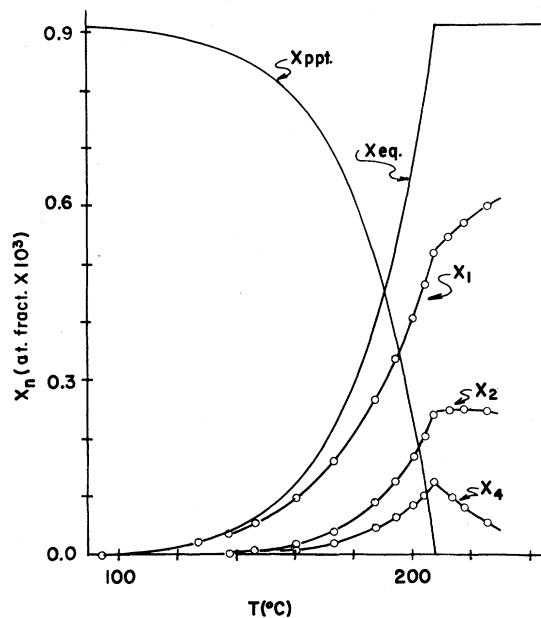


FIG. 3. A computation, using the CTW model, of expected concentrations of Au_1 's, Au_2 's, Au_4 's, and, through conservation of Au, of the Pb_3Au precipitate for the same temperatures as in Fig. 2.

Similarly, assuming no systematic error exists in $a_{\text{alloy}} - a_{\text{pb}}$, the $\Delta a/a$ per precipitated Au atom is obtainable from the room-temperature data after the precipitation anneal as -0.018 . Finally, the time dependence of $\Delta a/a$ seen in the 95–128°C region during precipitation suggests that Au must pass through some intermediate structure between Au_4 and Pb_3Au which causes lattice expansion. A possible candidate is, naturally Au_2 , since equilibrium considerations at these temperatures and concentrations indicate that it should appear in appreciable quantities. There is also some indication of this possibility from the equilibrium fitting attempts, described below, but a more detailed study will be required.

The equilibrium result (filled circles in Fig. 1) can be qualitatively understood in terms of the model of Cohen, Turnbull, and Warburton (CTW) which assumes thermodynamic equilibrium among three Au defect species: Au_1 's, Au_2 's and Au_4 's.⁶ Using the energies given by CTW and the solubility of Au in Pb (Fig. 2), we obtain the equilibrium concentrations of Au_1 , Au_2 , Au_4 , and Pb_3Au shown in Fig. 3. Comparison to the equilibrium portion of Fig. 1 shows that the initial downturn is primarily a result of the appearance of Au_1 (singlets), with the higher-temperature departure from exponential behavior resulting from increases in doublet and quadruplet concentrations. The

upswing following complete dissolution at 208°C implies, since $x_{\text{Pb}_3\text{Au}}=0$ and x_2 is approximately constant, that the Au_4 's cause a greater shrinkage than Au_1 's on a *per-atom* basis since the former are being converted into the latter in this region.

An attempt was made to quantify these observations by computer fitting the data using the CTW model and treating the strains per defect type as adjustable parameters. The model variables were $\Delta a/a_0$ for the *i*th defect (monomers, doublets, tetramers, Pb_3Au) and the linear thermal expansion coefficient for the Pb_3Au -induced change. The results are not particularly illuminating, however, being extremely sensitive to such additional assumptions as including the linear temperature dependence for the precipitate strain or considering that only data above 130°C are truly equilibrium data (filled circles in Fig. 1). Further, in all of the above cases, the strains obtained per Au_4 defect were between 2 and 5 times larger than the value in Eq. (2), with similar discrepancies for the Pb_3Au strains. While this suggests that the model may be deficient in all of the fits, the strains for both Au_1 and Au_4 defects were negative, with the Au_4 value typically significantly *larger* than Au_1 value per atom (in the two best fits 1.7 and 4.4 times larger). Au_2 values, on the other hand, were poorly defined, but more often showed positive rather than negative values, which would allow a straightforward interpretation of the data obtained during precipitation, as mentioned earlier.

These lattice-parameter results require a re-examination of the distribution of Au defects in Pb. Since the lack of noticeable curvature in an Arrhenius plot of the Au deenhancement results⁵ implies dominance of a single type of singlet, the assumption had hitherto been that these accounted for the observed extremely rapid diffusion. If another singlet species is to be present, this deenhancement result requires that it be strictly a minority constituent with a large free-energy difference from the principal singlet. However, considering the present $\Delta a/a$ result, it is extremely unlikely (essentially incorrect) that the defect which collapses the Pb lattice sits in an interstitial site, and we must now insist that *two* singlet species are present (in addition to Au_2 's and Au_4 's). In this view, which is essentially one of dissociative equilibrium,⁴ the primary singlets are more plausibly *substitutionals*, since the Au

Goldschmidt radius is smaller than that of Pb. Further, to be in accord with the deenhancement results noted above, essentially the entire enthalpy of diffusion, H_d , is required to produce the minority interstitial singlet population responsible for diffusion, implying that the enthalpy of motion H_m is essentially zero. This explanation has some attendant difficulties, however, since we must still presumably account for the formation of two additional defects, the Au_2 's and Au_4 's, which are both enthalpically more stable than a simple substitutional.⁶ Further, the structure of the Au_4 's will require reconsideration since it is also unlikely that an Au_4 tetrahedron occupying a Pb vacancy⁷ produces a larger lattice contraction than a single Au substitutional.

We thank Professor D. Turnbull for discussions of various phases of this work and Dr. T. H. Metzger for experimental assistance. One of us (W.K.W.) expresses his appreciation to the Robert A. Welch Foundation for a postdoctoral fellowship during his stay in Houston. We also thank the U. S. Department of Energy, Office of Basic Energy Sciences, for their support of our overall program on structural defects in solids.

^(a)Current address: Stanford Synchrotron Radiation Laboratory, Stanford University, Stanford, Cal. 94305.

¹W. Seith and H. Etzold, *Z. Elektrochem.* **40**, 829 (1934).

²N. L. Peterson, in *Solid State Physics*, edited by H. Ehrenreich, F. Seitz, and D. Turnbull (Academic, New York, 1965), Vol. 22, p. 409.

³T. R. Anthony, in *Vacancies and Interstitials in Metals*, edited by A. Seeger *et al.* (North-Holland, Amsterdam, 1970).

⁴W. K. Warburton and D. Turnbull, in *Diffusion in Solids: Recent Developments*, edited by A. S. Nowick and J. J. Burton (Academic, New York, 1975).

⁵W. K. Warburton, *Phys. Rev. B* **11**, 4945 (1975).

⁶B. M. Cohen, D. Turnbull, and W. K. Warburton, *Phys. Rev. B* **16**, 2491 (1977).

⁷A. N. Rossolimo and D. Turnbull, *Acta Metall.* **21**, 21 (1973).

⁸See, for example, H. Peisl, *J. Appl. Crystallogr.* **8**, 143 (1975).

⁹W. L. Bond, *Acta Crystallogr.* **13**, 814 (1960).

¹⁰*Handbook of Chemistry and Physics* (Chemical Rubber, Cleveland, 1972), p. D141.